Int. J. Heat Mass Transfer. Vol. 25, No. 11, pp. 1771–1773, 1982
Printed in Great Britain

0017-9310/82/111771-03 $03.00/0
Pergamon Press Ltd.

SOLIDIFICATION IN AN ANNULUS

T. K. SINHA and J. P. GUPTA*
Chemical Engineering Department, Indian Institute of Technology, Kanpur-208016, India

(*Received for publication* 25 *March* 1982)

NOMENCLATURE

a, radius of outer cylinder;
b, radius of inner cylinder;
C, specific heat;
k, thermal conductivity;
L, latent heat of fusion;
r, radial coordinate;
r_i, interface location, real;
r_a, interface location, apparent;
t, time;
T, temperature;
T_c, temperature of cold surface;
T_f, fusion temperature;
T_i, initial temperature;
T^*, dimensionless temperature;
X, dimensionless interface location.

Greek symbols

α, thermal diffusivity;
α_{sL}, ratio of solid to liquid phase thermal diffusivities;
β, ratio of inner to outer cylinder radii;
ε, modified Stefan number;
η, dimensionless radial coordinate in the liquid phase;
ξ, dimensionless radial coordinate in the solid phase;
ρ, density;
τ, dimensionless time;
ϕ_f, dimensionless initial liquid-phase temperature, $\left[\frac{k_L(T_i - T_f)}{k_s(T_f - T_c)}\right]$.

Subscripts

L, liquid phase;
s, solid phase.

INTRODUCTION

PHASE change problems, known generally as Stefan's problem, have been solved for over a century by various workers in a variety of geometrical configurations and boundary conditions [1, 2]. This includes the inward and outward solidification around an infinitely long cylinder. However, information on annular systems is conspicuously absent except for ref. [3] where the inward solidification of an annulus was analyzed by the perturbation technique. No experiments were performed. This problem is of importance in mold casting and solidification fouling. In the work reported here, we have experimentally studied the outward solidification in a concentric annulus where the initial temperature was above the freezing temperature. Then a set of equations was formulated for the problem. These equations were non-dimensionalized and the moving boundary was immobilized by coordinate transformation. These were then solved numerically and the results have been compared with the experiments.

EXPERIMENTAL SET-UP

A schematic diagram of the experimental set-up is shown in Fig. 1. It consists of a horizontal, 0.0125 m O.D. copper tube placed concentrically in a 0.051m I.D. glass pipe, 1m long. Refrigerant at a controlled, low temperature was circulated through the copper tube while the glass pipe was heavily insulated using glasswool and reflecting aluminum foil. The annular space was filled with distilled water at room temperature taking care to drive out all the air. The change in water volume due to changes in density was accommodated by connecting one end to a water-filled graduated burette whose level was periodically noted. The temperature of water as well as of the refrigerant was measured both near the inlet and the outlet as shown in Fig. 1. The thickness of the frozen layer of ice was measured periodically by a cathetometer with a least count of 1×10^{-5} m. Since the copper tube and ice were surrounded by water while the cathetometer was in the room air, the refractive index affected the readings. Using a geometrical technique (Fig. 2), a calibration curve was made between the apparent thickness of the ice layer as noted by the cathetometer and the real thickness (Fig. 3). This was used to obtain the actual thickness which has been plotted for different experiments in Fig. 4. τ_0 is the initiation time for freezing to start since $T_i > T_f$.

MATHEMATICAL FORMULATION

The energy balances in the solid and the liquid phases and at the interface, along with the initial and boundary conditions are given below

$$\frac{\partial T_s}{\partial t} = \alpha_s\left(\frac{\partial^2 T_s}{\partial r^2} + \frac{1}{r}\frac{\partial T_s}{\partial r}\right), \quad b < r < r_i(t), \tag{1}$$

$$\frac{\partial T_L}{\partial t} = \alpha_L\left(\frac{\partial^2 T_L}{\partial r^2} + \frac{1}{r}\frac{\partial T_L}{\partial r}\right), \quad r_i(t) < r < a. \tag{2}$$

The energy balance at the interface gives

$$k_s\frac{\partial T_s(r_i, t)}{\partial r} - k_L\frac{\partial T_L(r_i, t)}{\partial r} = \rho_L\frac{dr_i}{dt}, \quad r = r_i(t). \tag{3}$$

The initial and boundary conditions are

$$T_L(r, 0) = T_i, \tag{4}$$

$$T_s(b, t) = T_c, \tag{5}$$

$$T_s(r_i, t) = T_L(r_i, t) = T_f, \tag{6}$$

* To whom correspondence should be addressed.

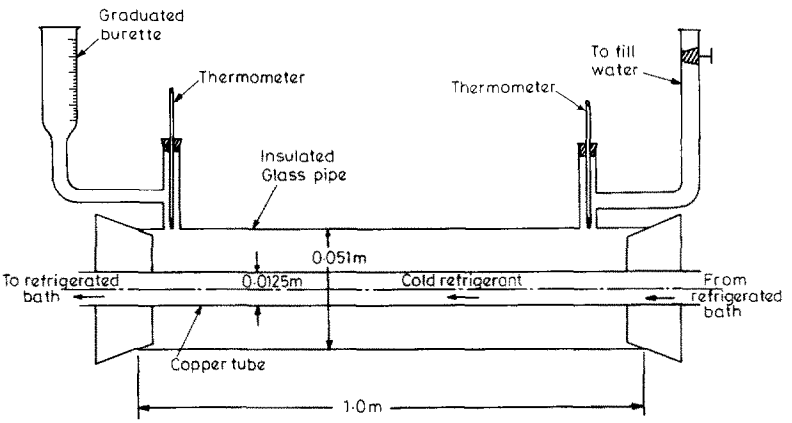

FIG. 1. Experimental set-up.

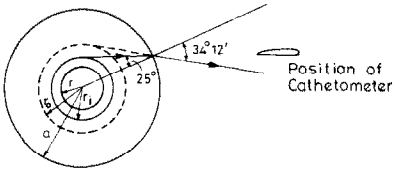

FIG. 2. Geometrical solution of refraction problem.

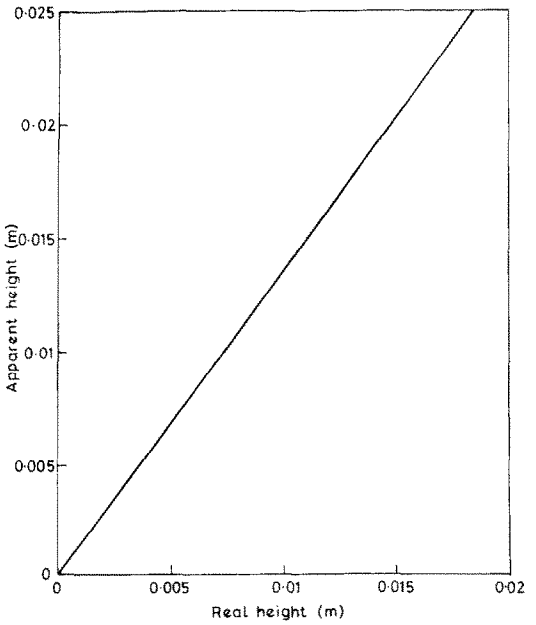

FIG. 3. Apparent height vs real height of solid front.

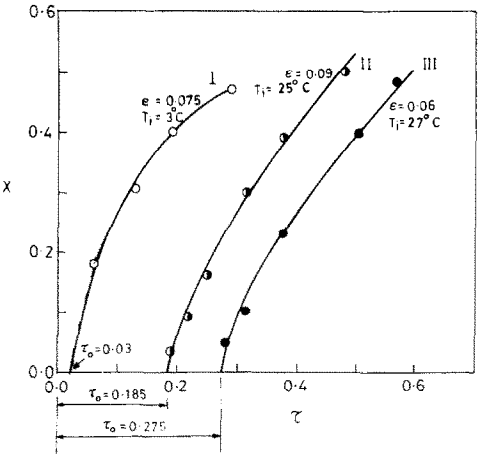

FIG. 4. Experimental X vs τ curves.

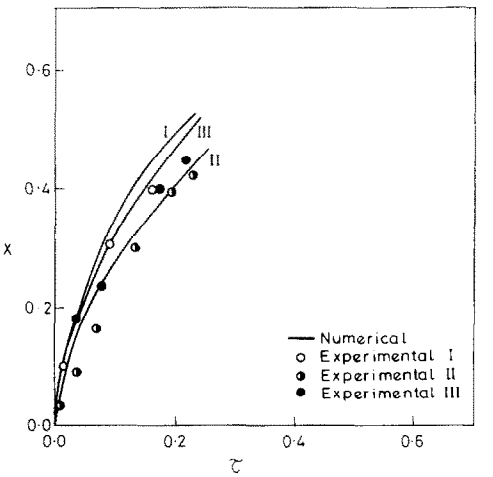

FIG. 5. Comparison between numerical and experimental results.

$$\frac{\partial T_L(a, t)}{\partial r} = 0. \quad (7)$$

The above are based on the assumptions of constant properties and pure conduction heat transfer.

To non-dimensionalize the equations and to immobilize the interface, the following parameters are used:

$$\eta = \frac{r_i(t) - r}{r_i(t) - a}, \quad (8)$$

$$\xi = \frac{r - b}{r_i(t) - b}, \quad (9)$$

$$T_s^* = \frac{T_s - T_c}{T_f - T_c}, \quad (10)$$

$$T_L^* = \frac{k_L(T_L - T_f)}{k_s(T_f - T_c)}, \quad (11)$$

$$\tau = \frac{v\alpha_s t}{a^2}, \quad (12)$$

$$\varepsilon = \frac{C_s(T_f - T_c)}{L}, \quad (13)$$

$$X = \frac{r_i(t) - b}{a}, \quad (14)$$

$$\alpha_{sL} = \frac{\alpha_s}{\alpha_L}, \quad (15)$$

$$\beta = \frac{b}{a}. \quad (16)$$

Using the above, the governing equations and the initial and boundary conditions get transformed to the following dimensionless form

$$\frac{\partial^2 T_s^*}{\partial \xi^2} + \frac{X}{\beta + \xi X}\frac{\partial T_s^*}{\partial \xi} = \varepsilon\left[X^2\frac{\partial T_s^*}{\partial \tau} - \xi X\frac{dX}{d\tau}\frac{\partial T_s^*}{\partial \xi}\right], \quad 0 < \xi < 1, \quad (17)$$

$$\frac{\partial^2 T_L^*}{\partial \eta^2} + \frac{1 - X - \beta}{[(\beta + X) + (1 - X - \beta)\eta]}\frac{\partial T_L}{\partial \eta} \times \alpha_{sL}\varepsilon\left[(1 - X - \beta)^2\frac{\partial T_L^*}{\partial \tau} - (1 - X - \beta)(1 - \eta) \times \frac{dX}{d\tau}\frac{\partial T_L^*}{\partial \eta}\right], \quad 0 < \eta < 1, \quad (18)$$

$$(1 - X - \beta)\frac{\partial T_s^*}{\partial \xi} - X\frac{\partial T_L^*}{\partial \eta} = X(1 - X - \beta)\frac{dX}{d\tau}, \quad (19)$$

$$T_s^*(0, \tau) = 0, \quad (20)$$

$$T_s^*(1, \tau) = 1, \quad (21)$$

$$T_L^*(0, \tau) = 0, \quad (22)$$

$$\frac{T_L^*(1, \tau)}{\partial \eta} = 0, \quad (23)$$

$$T_L^*(\eta, 0) = \phi_f. \quad (24)$$

SOLUTION TECHNIQUE

Equations (17)–(19) were solved by the implicit finite difference scheme. Equation (19), when written in the finite-difference form, reduced to a cubic polynomial which was solved by the method discussed by McCormick and Salvadori [4].

At time $\tau = 0$, the starting difficulties were avoided by assuming a very small thickness of the solid, $X = 0.0001$. Results obtained with $X = 0.0001$ were also checked by using $X = 0.0005$ and 0.001 respectively. No significant difference was obtained. The temperature profile in the solid was assumed to be linear at time $\tau = 0$ which has been assumed by many workers including Szekely and Stanek [5]. The next step involved in the computation was the simultaneous solution of equations (17) and (18). The liquid and the solid regions were divided into 10 grid spacings of equal width. Calculations were also carried out using 20 grid spacings and no significant difference was obtained. Since the implicit finite difference scheme is a standard one, further discussion here is avoided to save space. Its accuracy was checked by re-solving the inward solidification problem discussed in ref. [3].

RESULTS

The results obtained by the numerical solution of the equations are plotted in Fig. 5. Superimposed are the experimental results from Fig. 4 after subtracting respective τ_0 since the equations assume the freezing to start immediately while there is actually a finite time in each case during which only the sensible heat is removed and after which the actual freezing starts. The comparison of the results is satisfactory within the assumptions of the constant physical properties, pure heat conduction and experimental errors.

CONCLUSIONS

Experimental and numerical solutions for radially outward freezing in a concentric cylindrical annulus have been obtained and compared. The comparison shows that the numerical results can be taken as an upper bound on the location of the solidification front. The numerical scheme has also been used to correctly predict the effects of initial temperature and the cold wall temperature. These results have not been shown to save space.

Acknowledgement—This work was partly supported by Grant No. 12 (36)/78-SERC by the Department of Science and Technology, Government of India.

REFERENCES

1. S. G. Bankoff, Heat conduction or diffusion with change of phase, *Adv. Chem. Engng* **5**, 75 (1964).
2. J. P. Gupta, S. W. Churchill and N. Lior, Review of heat transfer with solidification/melting, to be published in *Adv. Heat Transfer*.
3. L. M. Jiji and S. Weinbaum, Perturbation solutions for melting or freezing in annular regions initially not at the fusion temperature, *Int. J. Heat Mass Transfer* **21**, 581 (1978).
4. J. M. McCormick and M. G. Salvadori, *Numerical Methods in Fortran*. Prentice-Hall, Princeton (1964).
5. J. Szekely and U. Stanek, Natural convection transients and their effects in unidirectional solidification, *Met. Trans.* **1**, 2243 (1970).